Journal of
Nanoscience and Nanotechnology
Vol. 11, 11200–11205, 2011

Influence of Structure Parameters and Crystalline Phase on the Photocatalytic Activity of TiO_2 Nanotube Arrays

Xuming Zhang[1, 2], Kaifu Huo[1, 2, *], Hairong Wang[1], Wenrui Zhang[1], and Paul K. Chu[2, *]

[1] *The Key State Laboratory Breeding Base of Refractories and Ceramics, School of Materials and Metallurgy, Wuhan University of Science and Technology, Wuhan 430081, China*
[2] *Department of Physics and Materials Science, City University of Hong Kong, Tat Chee Avenue, Kowloon, Hong Kong, China*

Titanium oxide nanotube arrays (TiO_2–NTAs) with different diameters and lengths are prepared by anodization of titanium foils in a water/ethylene glycol solution (5:95 V/V) containing 0.3 wt% NH_4F. The effects of the diameters, lengths and crystalline phases of the NTAs on the photocatalytic (PC) activity are systematically evaluated. Larger pore diameter results in higher PC activity. The PC activity increases initially and then decreases with lengths for TiO_2–NTAs and the optimal length that yields the highest PC activity is observed to be 6.2 μm. The crystalline phase and corresponding PC activity depend on the calcination temperature and their relationship is also investigated. The amorphous-to-anatase and anatase-to-rutile phase transitions initially occur at 300 and 500 °C, respectively. The PC activity of TiO_2–NTAs initially increases with calcination temperature from 250 to 500 °C and then decreases at higher calcination temperature. The enhanced PC activity observed from the samples annealed at 250-450 °C is attributed to the better anatase crystalline structure at higher calcination temperature. The highest PC activity with regard to photodecomposition of methyl orange is observed from TiO_2–NTAs calcined at 500 °C, which coincides with the anatse-to-rutile phase transformation. The synergistic effect of the anatase TiO_2–NTAs and rutile barrier layers facilitate interfacial electron transfer consequently enhancing the PC activity. Further elevation of the calcination temperatures to 550 and 600 °C exhibits diminished PC activity because the NTs become shorter due to conversion of the bottom of anatase NTs into rutile film.

Keywords: TiO_2, Nanotube Arrays, Length, Pore Size, Crystalline Phase, Photocatalysis.

RESEARCH ARTICLE

1. INTRODUCTION

Titanium dioxide (TiO_2) has been widely used in photodecomposition of organic contamination because of its high photosensitivity, strong oxidizing activity, as well as biological and chemical stability.[1, 2] The nanosized TiO_2 photocatalyst used in environmental control has been mainly suspended zero-dimensional (0D) nanoparticles,[3, 4] but post-treatment recovery of the catalyst is very difficult and expensive. Immobilization of TiO_2 nanoparticles has been carried out on different substrates to circumvent,[5, 6] but unfortunately, the photocatalytic (PC) efficiency of the immobilized system is much lower than that of the corresponding slurries due to the inevitably reduced surface area associated with nanoparticle immobilization prolonging the photodegradation time.[7, 8] One effective approach to enhance the PC activity is to fabricate one-dimensional (1D) nanostructured TiO_2 photocatalysts, especially substrate-anchored 1D TiO_2 nanotube arrays (TiO_2–NTAs), which provide large active surface areas without the inherent drawback of particle immobilization. At the same time, a large active surface area and multiple diffusion pathways in the NTAs enable ready access to the TiO_2 surface by reactants and easy release of photoreaction products. Anodization is a relatively simple and efficient method to fabricate TiO_2–NTAs on Ti substrates such as sheets, foils, wires, and so on.[9–11] Since the first report on TiO_2–NTAs fabricated by potentiostatic anodization of a Ti foil by Gong et al.,[12] TiO_2–NTAs have attracted increasing attention in photodegradation of environmental pollutants.

Recent investigations suggest that the PC activity of TiO_2–NTAs depends very much on their structures such as lengths, pore diameters and crystalline phase composition.[13, 14] Larger diameter NTs can photodegrade pollutants more quickly due to the improved accessibility to pollutants. Longer NTs have larger surface areas enabling more light harvesting and larger active sites accessible to pollutants in the aqueous environment. These

*Authors to whom correspondence should be addressed.

 1533-4880/2011/11/11200/006 doi:10.1166/jnn.2011.4074

factors lead to a higher PC activity.[10, 15] However, light harvesting by the TiO_2–NTAs does not necessarily increase when the length of the TiO_2–NTAs exceeds a certain value because the light intensity is usually attenuated sharply as it penetrates the solid photocatalyst film.[16, 17] Thus, there should be an optimal length and diameter for the highest PC activity. In addition, the crystalline phases in the TiO_2–NTAs impact the PC activity. Some researchers allege that TiO_2–NTAs with the anatase structure have a higher PC activity,[18] but there have been counter results suggesting that the mixed anatase and rutile structure yields the best PC properties.[19, 20] Although there have been some reports on the relationship between the structure or crystalline phase and PC properties of TiO_2–NTAs,[15, 17] the effects of the NT structural parameters and crystalline phase composition on the PC activity have not been investigated in details and systematically and this is motivation of the work presented here.

2. EXPERIMENTAL DETAILS

Titanium foils (0.5 mm thickness, 99.6% purity) were purchased from Aldrich. Anodization reaction was carried out in a conventional two-electrode cell equipped with a direct current (DC) power supply (IT6834, ITECH, China). The Ti foil served as the anode electrode and a graphite foil as the counter electrode (1 cm separation). The electrolyte was ethylene glycol containing 0.3 wt% ammonium fluoride (NH_4F) and 5 vol% distilled (DI) water. After anodization, the samples were rinsed with DI water several times and dried in air. The as-anodized NTAs initially had an amorphous structure and could be calcined to convert to crystalline NTAs. The morphology, structure, and composition of the TiO_2–NTAs were determined by field-emission scanning electron microscopy (FE-SEM, FEI Nova 400 Nano), X-ray diffraction with Cu K_α radiation ($\lambda = 1.5416$ Å) (XRD, Philips X' Pert Pro), and Micro-Raman spectra (Renishaw 2000 Raman spectrometer). The thickness of the NT film was estimated directly from the cross-section SEM image.

The PC activity of the as-prepared TiO_2–NTAs with a size of 1×1 cm^2 was measured using 20 ml of methyl orange (MO) aqueous solution with an initial concentration of 10 mg/L as the probing solution. The MO solution was stirred in dark for 2 hrs to saturate the photocatalyst with MO molecules. The photodegradation experiments were performed at the natural pH of the MO dye and the solution was aspirated continuously with air during the PC reaction. A high pressure mercury lamp (500 W, primary wavelength of 365 nm) was used as the UV irradiation source. The average UV intensity impacting the samples surface was 4.0 mW/cm^2 measured by an irradiance meter (Model: UV-A, Beijing Normal University, China). The change in the MO concentration with time was monitored using a UV-Vis spectrophotometer (TU-1810SPC, Beijing PGENERAL, China).

3. RESULTS AND DISCUSSION

Figures 1(a–c) show the top and side FE-SEM images of the samples prepared in NH_4F-ethylene glycol at 20, 40 and 60 V for 2 hrs demonstrating that uniform NTAs have been fabricated on the Ti foil. In addition, the length and diameter of NTAs increase with a higher voltage. At 20 V for 2 hrs, 1.3 μm long NTAs with a diameter of about 50 nm are produced (Fig. 1(a)). When the anodization voltage is increased to 40 V for 2 hrs, the diameter enlarges to 90 nm (Fig. 1(b)) and the NTAs lengthen to 3 μm. A higher voltage of 60 V for 2 hrs produces NTAs with a diameter of 120 nm and length of 9.4 μm (Fig. 1(c)). Figure 1(d) presents the relationship between the length and diameter of the NTAs and voltage for 2 hrs anodization time, indicating that the diameter increases almost linearly with the voltage, but the length increases dramatically when voltage is over 40 V. The anodization time also plays an important role in the surface morphology, pore size, and length of the NTAs. Figure 1(e) depicts the evolution of the pore size and length of NTs with anodization time at 40 V. Although the NTAs lengthen dramatically with anodization time, the diameters of NTAs do not obviously increase with time.

Figure 2(a) shows the static absorption curve of the Ti foil and as-anodized 4.5 μm long NTAs with different diameters (50, 90 and 120 nm) synthesized at 20 V, 40 V, and 60 V for anodization time of 7 hrs, 3 hrs and 1 hr. The samples 1×1 cm^2 in size are immersed in 4 mL MO with an initial concentration of 5 mg/L in dark and the absorbance is measured every 15 minutes. As shown in Figure 2(a), NTAs with a larger pore diameter have stronger adsorption ability. After 80 minutes, the absorbance remains unchanged implying that absorption and desorption of MO on the TiO_2–NTAs is in equilibrium. The PC activity of the specimens is evaluated using MO in the aqueous solution as the probing molecule under UV illumination. The MO solution is stirred in dark for 2 hrs to saturate the photocatalyst with MO molecules. Direct photolysis is then carried out without using the photocatalyst. Figure 2(b) is the plot of the concentration of MO in the aqueous solution versus UV illumination time, showing that the PC activity is enhanced as the pore diameter of the NTAs increases.

We have evaluated the effect of the length of the NTAs on the PC activity, the photodegradation of MO in the aqueous solution is studied by UV irradiation in the presence of the NTAs samples. The anatase NTAs with a diameter of 90 nm and lengths of about 1.2, 3, 6.2 and 10 μm are employed to investigate the PC activity dependence on nanotubes length. Figure 3(a) plots the concentration of MO in the aqueous solution against UV illumination time. It can be clearly seen that the PC activity of TiO_2–NTAs increases initially as the length increases from 1.2 to 6.2 μm and then slightly decreases for longer NTAs (10 μm). The fastest PC degradation of MO is observed

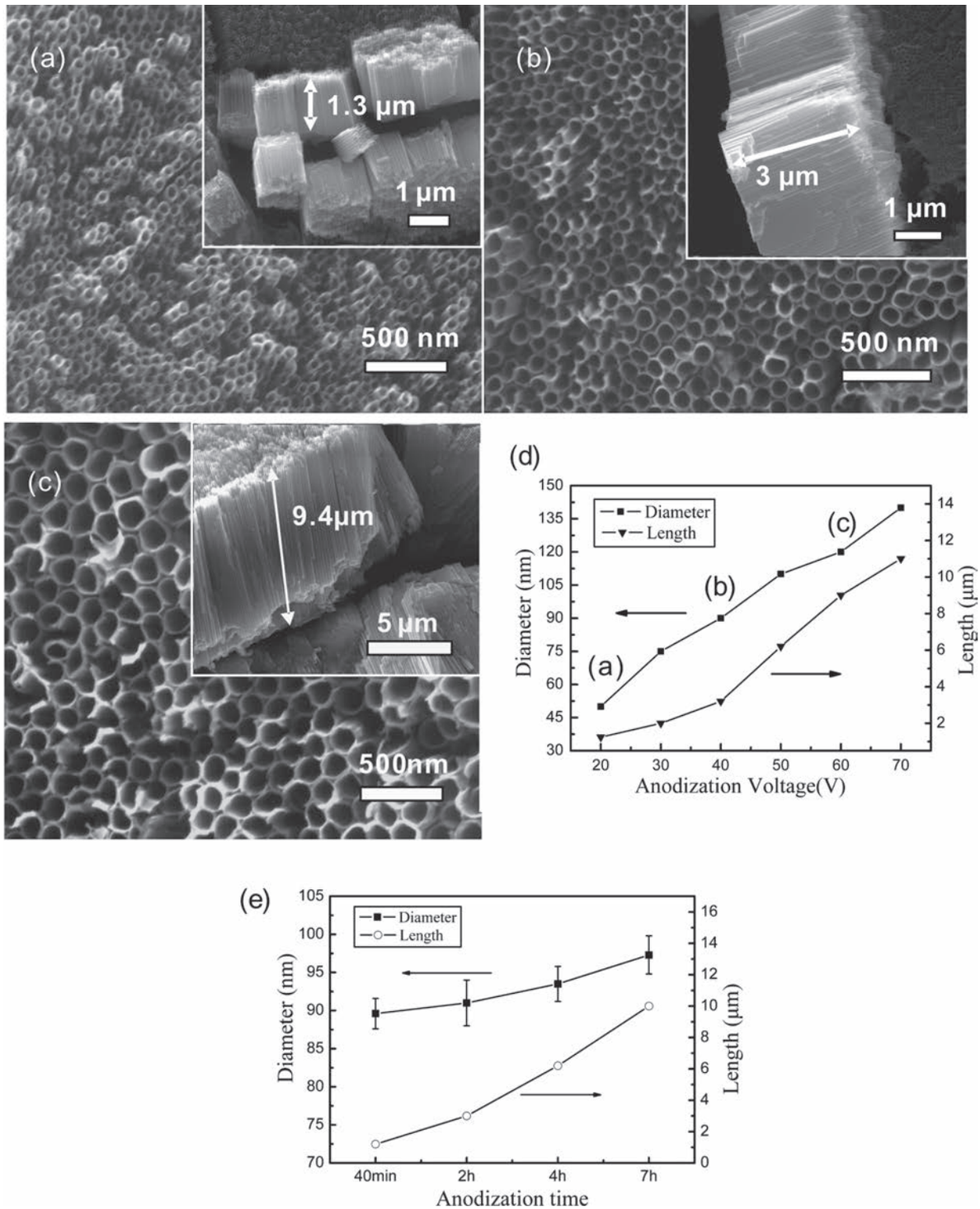

Fig. 1. Top-view and side-view FE-SEM images of the NTAs prepared at different voltage for 2 h: (a) 20 V, (b) 40 V. (c) 60 V. (d) Changes in length and diameter with anodization voltage for 2 hours duration. (e) Evolution of pore size and length of NTs with anodization time at 40 V.

from the 6.2 μm long NTAs and almost 90% of the MO is photodegraded within 180 min, suggesting that the tube length plays an important role in the PC activity of the TiO_2–NTAs.

In addition to NT dimensions, the crystalline phase compositions of the NTs are known to significantly influence PC activity. Since the as-anodized NTAs are amorphous, post-synthesis thermal calcination offers a powerful route

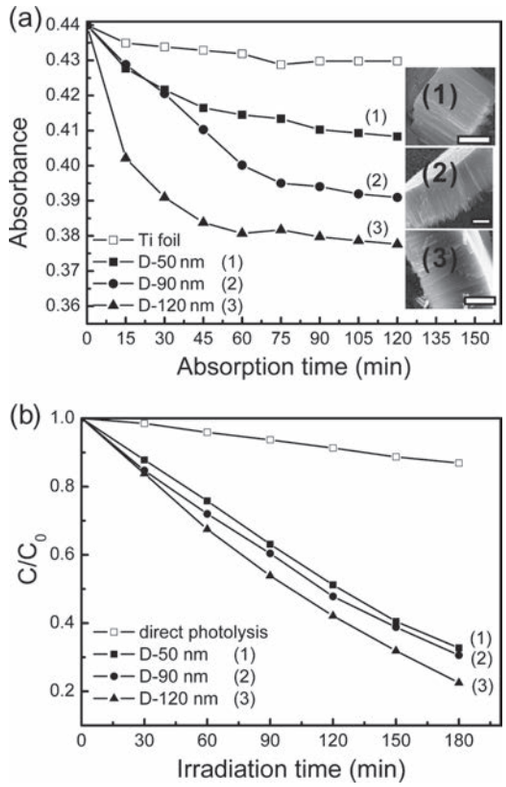

Fig. 2. (a) Static absorption curve of Ti foil and as-anodized NTAs with 4.5 μm length and different diameters. (b) Concentration (C) changes of methyl orange (MO) in aqueous solution as a function of illumining time (t) under UV light in the presence of 4.5 μm length NTAs.

to manipulate the TiO_2 crystalline characteristics, in particular, transformation from one crystalline phase to another. Figure 4(a) shows XRD patterns of NTAs with a diameter about 90 nm and length 6.2 μm cailcined at different temperature from 250 to 700 °C for 3 hrs in air. It can be seen that the as-anodized NTAs and NTAs calcined at 250 °C exhibit a featureless profile except the signals

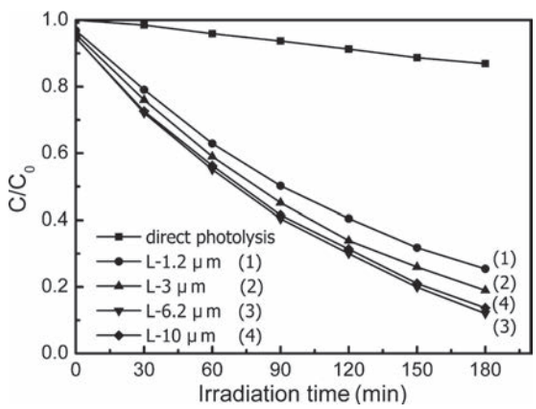

Fig. 3. (a) Concentration (C) changes of methyl orange (MO) in the aqueous solution as a function of illumining time (t) under UV light on NTAs with different lengths (1.2, 3, 6.2 and 10 μm).

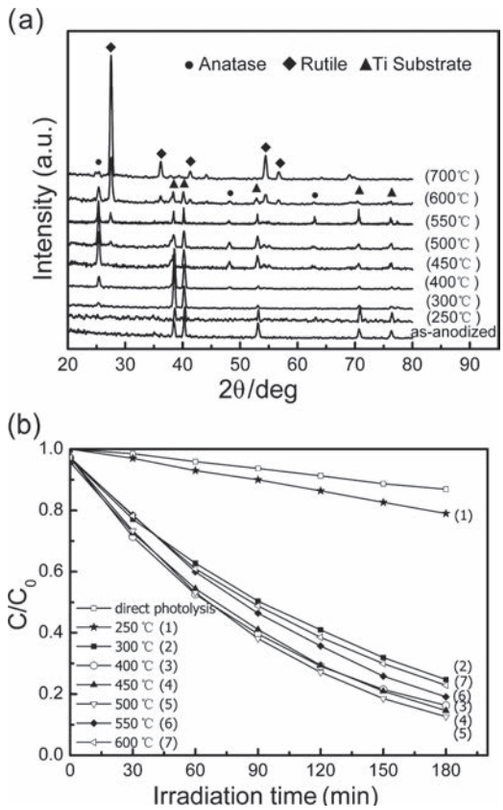

Fig. 4. (a) XRD patterns of TiO_2–NTAs annealed at temperatures ranging from 250 to 700 °C for 3 hrs (b) Concentration (C) changes of methyl orange (MO) in the aqueous solution as a function of illumining time (t) under UV light in the presence of NTAs calcined at different temperatures.

from the underlying Ti substrate, suggesting that the NTAs are amorphous. Crystallization of anatase TiO_2 occurs at 300 °C and the relative intensities of the anatase peaks increase with calcination temperature from 300 to 450 °C. By increasing the calcination temperature to 500 °C, several diffraction peaks characteristic of the rutile phase start to appear and it becomes the predominant crystal phase at 700 °C. The PC activity of the TiO_2–NTAs calcined at different temperatures is also evaluated by decomposition of MO during UV irradiation. Figure 4(b) depicts the decay profiles of MO absorption with photodegradation time in the presence of TiO_2–NTAs calcined from 250–600 °C. The samples annealed at over 300 °C show apparent enhanced PC activity compared to the amorphous sample and the PC activity increases with calcination temperature from 300 to 500 °C. Further elevation of the calcination temperature to 550 and 600 °C actually reduces the reaction rate constant. The highest PC activity as indicated by photodecomposition of MO is achieved from TiO_2–NTAs annealed at 500 °C for 3 hrs in air and it coincides with the anatase-to-rutile phase transition as shown in Figure 4(a).

Yang and coworkers [21] have investigated the crystallization and phase transition mechanism of TiO_2–NTAs. They

RESEARCH ARTICLE

conclude that the NTAs retain their anatase phase during the calcination process until the collapse of the nanotubular structure and the growth of the rutile thick film between the NTs and Ti supporting substrate and the decrease in the length of the anatase NTs are responsible for the changes in the XRD intensities of the anatase and rutile phases. We have also investigated the change in the length and morphology with calcination temperatures To observe the effects of the length in more details, 13.6 μm long NTAs are prepared by anodization of a Ti foil under 60 V for 3 hrs. As shown in Figure 5(a), the lengths of the NTAs calcined between 300 and 450 °C have no obviously changes in comparison with the as-anodized amorphous NTs. At 500 °C, the anatase to rutile phase transformation occurs and the length of the NTs slightly decreases to 12.6 μm. However, calcination at higher temperature between 550 and 600 °C causes the length of the nanotubes to decrease dramatically to 10.1 and 6.6 μm, respectively. Raman spectra (not shown here) suggest that all the calcined NTs show the vibration modes of anatase but no rutile signals. The glancing angle XRD pattern (not shown here) also confirms that the TiO_2 nanotubes still retain the anatase phase even after calcination at 600 °C for 3 hrs.

Crystallization of the anatase phase from amorphous TiO_2 occurs at 300 °C as shown in Figure 4(a). Initial

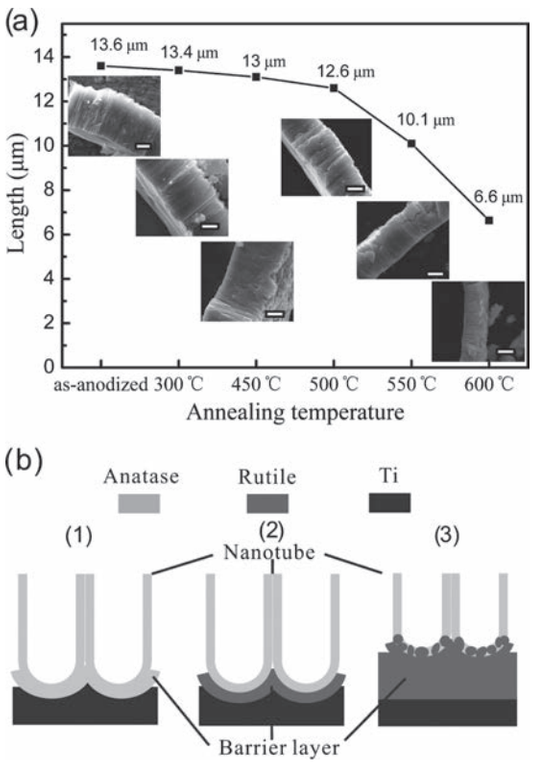

Fig. 5. (a) Evolution of length of NTAs at different calcination temperatures from 300 to 600 °C for 13.6 μm long NTAs. The insets are corresponding profile images and the scale bar is 5 μm. (b) Schematic of the TiO_2–NTAs annealed at (1) 450 °C, (2) 500 °C and (3) 600 °C in air.

crystallization of the anatase phase occurs both in the nanotubes and the barrier layer (the nanotube/Ti supporting interface) at almost the same temperature.[21, 22] When the calcination temperature is raised from 300 to 450 °C, the relative intensities of the anatase peaks increase and the anatase phase is well crystallized at 450 °C. During crystallization of the anatase phase the length and average diameter of the nanotubes do not change appreciably because there is not a big volume change between the amorphous and anatase phases.[21] The crystallized TiO_2–NTAs shown in Figure 5(b1) consist of well-crystalline anatase NTs and barrier layers. Since the crystallized anatase TiO_2 has fewer combination centers for the photogenerated carriers in comparison with amorphous TiO_2 the PC activity of the TiO_2–NTAs is enhanced when calcined between 300 to 450 °C. At 500 °C, the rutile phase emerges (see the XRD pattern in Fig. 4(a)) implying that the anatase-to-rutile transition occurs. Rutile nucleation first occurs in the barrier layer and does not take place easily inside the walls of the nanotubes due to the constraints imposed by the walls.[21, 22] Hence, the rutile barrier layer is formed but the anatase TiO_2–NTAs are retain, as shown in Figure 5(b2). It is well known that anatase TiO_2 (A) and rutile TiO_2 (R) have different band gaps (3.2 eV for anantase and 3.0 eV for rutile). Since the conduction band (CB) edge of anatase TiO_2(A) is about 0.2 eV higher than that of rutile TiO_2 (R), electrons can be transfer from the CB of TiO_2(A) to TiO_2(R) when TiO_2(A) and TiO_2(R) are close together.[23] This synergistic effect is believed to facilitate interfacial electron transfer thereby enhancing the PC activity and it is similar to that observed from ZnO/TiO_2 and CdS/ZnO composite photocatalysts.[24, 25] The TiO_2–NTAs calcined at 500 °C exhibits better PC activity compared to that calcined at 450 °C. However, if the calcination temperature is raised to 550 or 600 °C, rutile crystallites begin to grow along the anatase NTs and gradually merge the anatase NTs finally producing a rutile thick film by consuming the bottom layer of the NTs. This results in a dramatic decrease in the length of the NTs as shown in Figures 5(a and b3). Actually, the length of the NTAs calcined at 600 °C is about half that of the NTs annealed at 450 °C as shown in Figure 5(a). The smaller length decreases the surface area of the TiO_2 photocatalyst and hence, a higher calcination temperature (550 °C to 600 °C) leads to a smaller reaction rate constant as shown in Figure 4(b).

4. CONCLUSION

TiO_2–NTAs with different pore diameters and lengths are fabricated on Ti substrate by electrochemical anodization and the effects of the pore diameters and lengths on the PC activity are systematically evaluated. Larger pore diameter results in higher PC activity and PC activity increases initially and then decreases with lengths The as-anodized

NTAs are amorphous and can be crystallized by calcination in air. The amorphous-to-anatase and anatase-to-rutile phase transitions start to occur at 300 and 500 °C, respectively. The PC activity of the TiO_2–NTAs increases from 250 to 500 °C and then decreases at higher calcination temperature. The enhanced PC activity observed from samples calcined between 250 and 450 °C is caused by the more antase content. However, if the calcination temperature is higher than 500 °C, the NTs become shorter due to conversion of the bottom of anatase NTs into rutile film and decreased PC activity is observed. The highest PC activity is accomplished from TiO_2–NTAs calcined at 500 °C and this coincides with the anatse-to-rutile phase transformation. The anantse TiO_2–NTAs and rutile barrier layers facilitate interfacial electron transfer thereby enhancing the PC activity. The results reported here enable better understanding of the PC activity of NTAs film with different structures prepared at different calcination temperature.

Acknowledgments: This work was jointly supported by National High Technology Research and Development Program of China No. 2009AA02Z416, National Natural Science Foundation of China No. 50902104, Hubei Province Natural Science Foundation No. 2010CDB03402, Hong Kong Research Grants Council (RGC) General Research Funds (GRF) No. CityU 112307.

References and Notes

1. E. Y. Kim, J. H. Park, and G. Y. Han, *J. Power. Sources.* 184, 284 (**2008**).
2. A. Zhang, M. H. Zhou, L. Liu, W. Wang, Y. L. Jiao, and Q. X. Zhou, *Electrochim. Acta.* 55, 5091 (**2010**).
3. L. Andronic and A. Duta, *Mater. Chem. Phys*. 112, 1078 (**2008**).
4. S. Yurdakal, V. Loddo, B. B. Ferrer, G. Palmisano, V. Augugliaro, J. G. Farreras, and L. Palmisano, *Ind. Eng. Chem. Res.* 46, 7620 (**2007**).
5. P. E. DeJongh and D. Vanmaekelbergh, *Phys. Rev Lett* 77, 3427 (**1996**).
6. X. L. Liu, Y. F. Gao, C. X. Cao, H. J. Luo, and W. Z. Wang, *Langmuir.* 26, 7671 (**2010**).
7. M. F. J. Dijkstra, A. Michorius, H. Buwalda, H. J. Panneman, J. G. M. Winkelman, and A. A. C. M. Beenackers, *Catal. Today.* 66, 487 (**2001**).
8. M. Noorjahan, M. P. Reddy, V. D. Kumari, B. Lavedrine, P. Boule and M. Subrahmanyam, *J. Photochem. Photobiol. A* 156, 179 (**2003**).
9. J. Wang and Z. Q. Lin, *J. Phys. Chem. C* 113, 4026 (**2009**).
10. Z. Y. Liu, and M. Misra, *ACS Nano.* 4, 2196 (**2010**).
11. H. M. Liu, D. A. Wang, L. Ji, J. B. Li, S. J. Liu, X. Liu, and S. X. Jiang, *J. Chromatogr. A* 1217, 1898 (**2010**).
12. D. W. Gong, C. A. Grimes, O. K. Varghese, W. C. Hu, R. S. Singh, Z. Chen, and E. C. Dickey, *J. Mater. Res.* 16, 3331 (**2001**).
13. G. K. Mor, O. K. Varghese, M. Paulose, K. Shankar, and C. A. Grimes, *Sol. Energy. Mater. Sol. Cell.* 90, 2011 (**2006**).
14. H. F. Zhuang, C. J. Lin, Y. K. Lai, L. Sun, and J. Li, *Environ. Sci. Technol.* 41, 4735 (**2007**).
15. Y. R. Smith, A. Kar, and V. Subramanian, *Ind. Eng. Chem. Res.* 48, 10268 (**2009**).
16. H. T. Chang, N. Wu, and F. Zhu, *Water Res.* 34, 407 (**2000**).
17. H. C. Liang and X. Z. Li, *J. Hazard. Mater.* 162, 1415 (**2009**).
18. M. R. Hofmann, S. T. Martin, W. Choi, and D. W. Bahnemann, *Chem. Rev*. 95, 69 (**1995**).
19. G. Liu, X. X. Yan, Z. G. Chen, X. W. Wang, L. Z. Wang, G. Q. Lu, and H. M. Cheng, *J. Mater. Chem.* 19, 6590 (**2009**).
20. R. B. Zheng, X. W. Meng, and F. Q. Tang, *Appl. Surf. Sci.* 255, 5989 (**2009**).
21. Y. Yang, X. Wang, and L. Li, *J. Am. Ceram. Soc.* 91, 632 (**2008**).
22. O. K. Varghese *J. Mater. Res.* 18, 156 (**2003**).
23. D. C. Hurum, A. G. Agrios, K. A. Gray, T. Rajh, and M. C. Thurnauer, *J. Phys. Chem. B* 107, 4545 (**2003**).
24. D. Chen, H. Zhang, S. Hu, and J. H. Li, *J. Phys. Chem. C* 112, 117 (**2008**).
25. X. F. Gao, W. T. Sun, Z. D. Hu, G. Ai, Y. L. Zhang, S. Feng, F. Li, and L. M. Peng, *J. Phys. Chem. C* 113, 20481 (**2009**).

Received: 30 December 2009. Revised/Accepted: 30 August 2010.

RESEARCH ARTICLE